Chapter 3. High efficiency GaAs/Si three-terminal monolithic tandem solar cells

3-1 Introduction

The utilization of tandem solar cells can greatly increase the conversion efficiency, such as $Al_{0.37}Ga_{0.63}As$/GaAs (27.6%, AM1.5)[1] and GaInP/GaAs (29.5%, AM1.5) tandem solar cell,[2] because tandem solar cells converts a large fraction of the incident sunlight into electricity. It produces a wider photovoltaic spectral response region compared with a single-junction cell. GaAs/Si tandem solar cells have attracted attention as the most effective approach to achieve a high-efficiency solar cell with efficiency over 30% [3] on a large-area substrate. They are not only of high-efficiency and large-area but also have advantages in terms of cost, weight and mechanical strength. A high-efficiency (18.3%, AM0) GaAs single-junction solar cell on Si has been obtained by M. Yamaguchi[4]. GaAs film is highly transparent to infrared light of wavelengths beyond 0.87 μm. Using tandem-configuration, GaAs/Si solar cell with two-junction has a wider photovoltaic response in the long wavelength region compared with GaAs/Si single junction solar cell.

For 2-terminal monolithic GaAs/Si tandem solar cell, it is necessary to make the photocurrent matching between the top cell and bottom cell. Otherwise, the conversion efficiency will be decreased because the total photocurrent of GaAs/Si tandem solar cell is the smaller one of the top cell and bottom cell. Normally, the short-circuit current density (*Jsc*)

of the GaAs top cell is two times larger than that of the Si bottom cell.

We propose GaAs/Si monolithic 3-terminal cascade solar cell, which consists of a p^+-n GaAs top cell and an n^+-p Si bottom cell. For the 3-terminal model, it is not necessary to consider the photocurrent matching between the top cell and bottom cell and it is easy to make the best use of the incident sun light to be converted to electrical power. Three-terminal monolithic p^+-n AlGaAs/n^+-p Si solar cells are reported in the previous work [5].

There are high density of dislocations in GaAs heteroepitaxial film on Si substrate, which can act as the recombination centers. It results in the decrease of the conversion efficiency. This study describes the improvement of quantum efficiency and the increase of conversion efficiency for the top GaAs solar cell using the thermal treatment and using a graded-bandgap-emitter-layer (GBEL) of $Al_xGa_{1-x}As$. The effects of GaAs growth on the Si bottom cell are investigated, and the improvement of quantum efficiency of the Si solar cell in the long wavelength region using the back surface field (BSF) and p-Si substrate of high resistance are presented.

3-2 Sample fabrication

3-2-1 Si bottom cell

The substrates used for this study are 350 μm-thick single-side polished (100) 2° off towards [011] (resistivity is 0.1～ 10 Ω-cm) Czochralski (CZ) silicon wafers. The structure of n^+-p-p^+ Si were formed with P-thermal diffusion at 900 ℃ and B-thermal diffusion at 1000 ℃, respectively, using the spin coating method for the diffusion sources. The carrier concentration and depth of n^+ Si layer are 2.6×10^{19} cm^{-3} and 1.1 μm, respectively. The thickness of p^+ Si is 0.5 μm. The measurements were made by the four-point probe method and the electron beam induced current method (EBIC), respectively.

3-2-2 GaAs top cell

After the n^+-p-p^+ Si sample was formed, it is used as a substrate for GaAs solar cell in an atmospheric pressure metalorganic chemical vapor deposition (MOCVD) equipment. The two-step growth method and in-situ thermal cycle annealing (TCA) were adopted[6),7)]. Before GaAs growth, the high-temperature heating of 1000 ℃ was done for 5 minutes so as to clean the Si substrate. During the growth of 2 μm-thick GaAs layer, TCA from 300 ℃ to 900 ℃ was carried out 5 times to improve the quality of GaAs film on Si. Three kinds of growth sequences for the GaAs top cell were adopted. These are shown in Fig.3-1. The differences in the sequences are the temperature of the thermal cycle annealing (TCA) and growth of

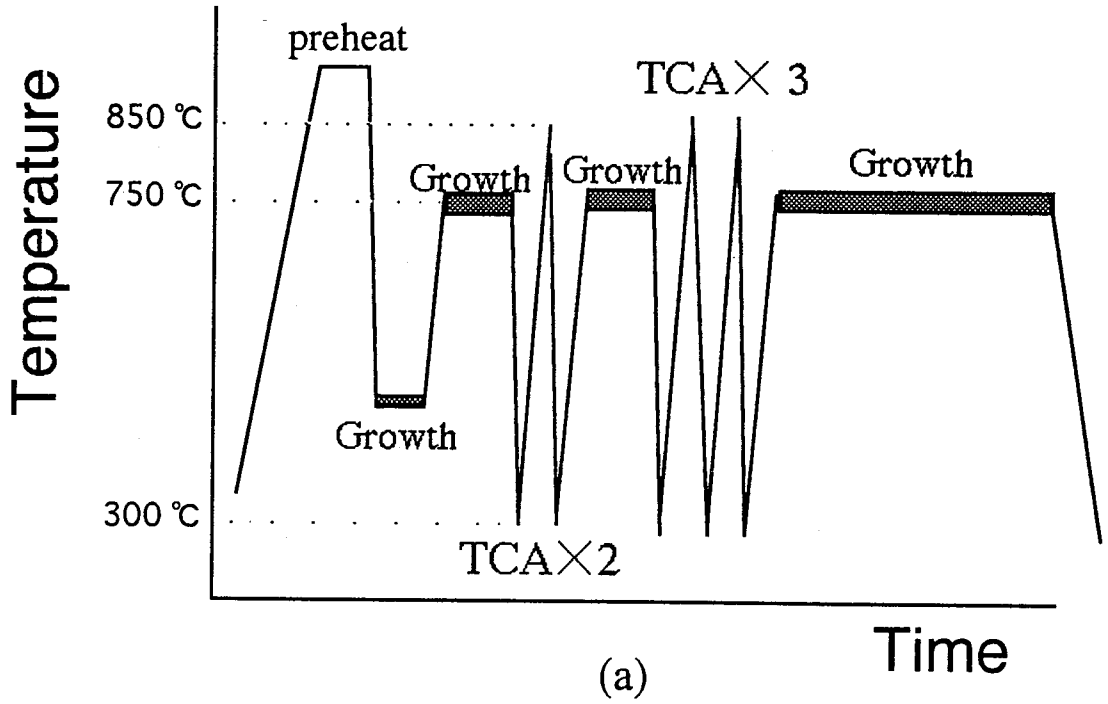
Temperature
preheat
850 ℃
750 ℃
300 ℃
Growth
Growth
Growth
Growth
TCA× 3
TCA×2
Time

(a)

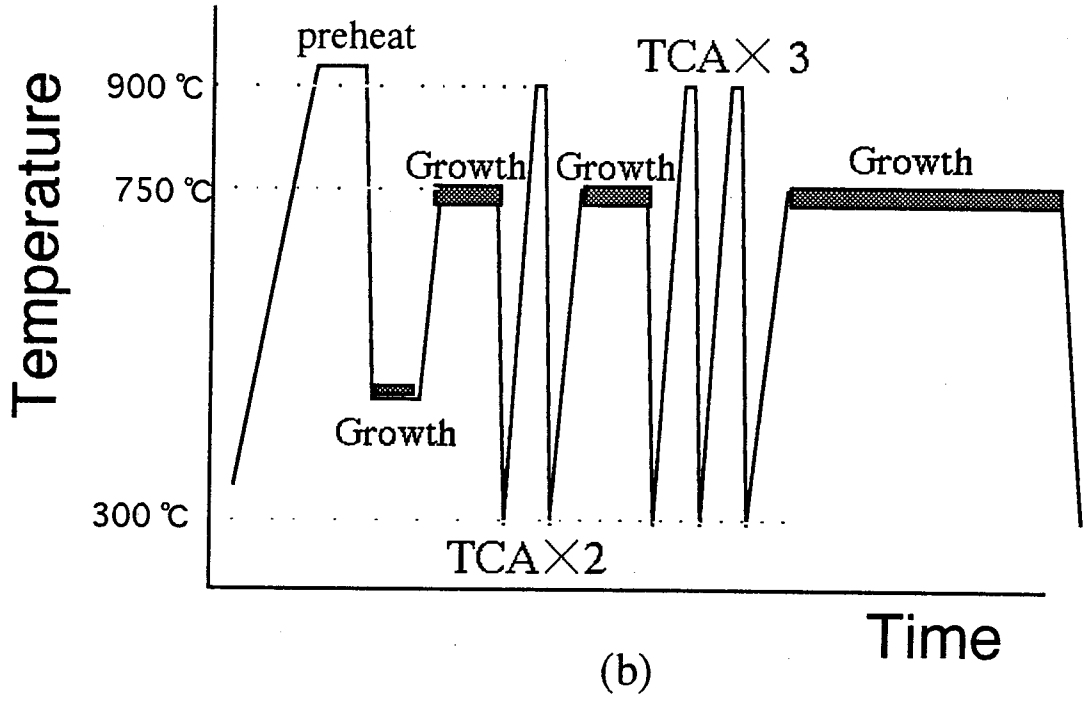
Temperature
preheat
900 ℃
750 ℃
300 ℃
Growth
Growth
Growth
Growth
TCA× 3
TCA×2
Time

(b)

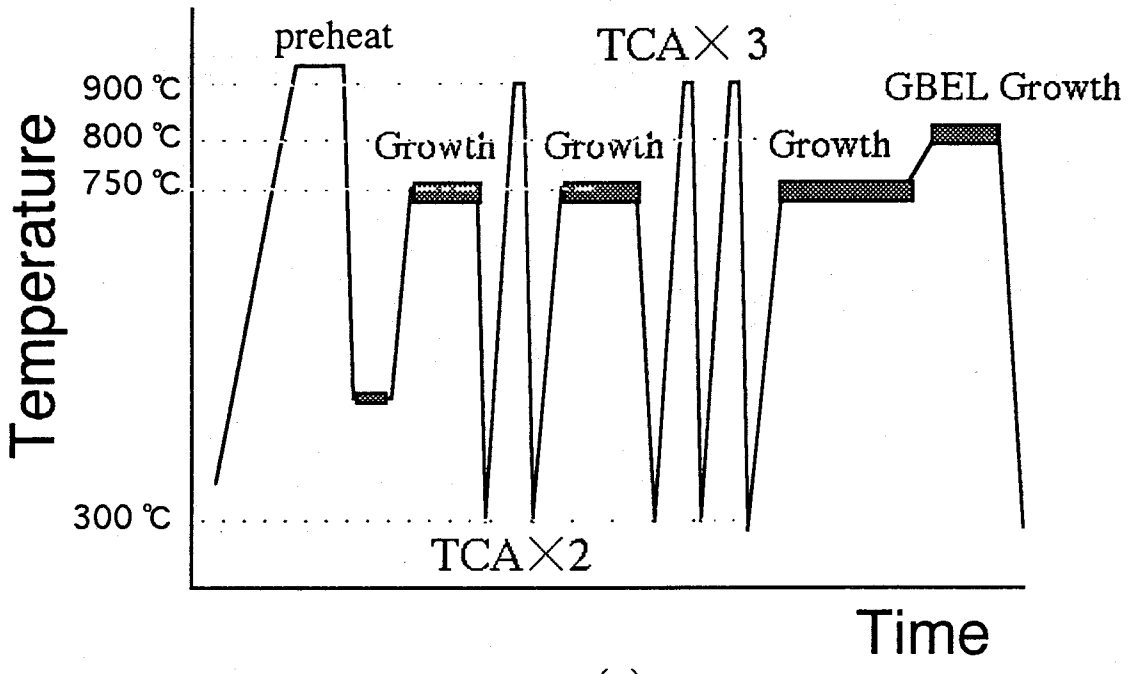

(c)

Fig.3-1 The growth sequences of GaAs solar cells on Si.

sequence (a) : 300~850 ℃ (TC×5);
sequence (b) : 300~900 ℃ (TC×5);
sequence (c) : 300~900 ℃ (TC×5)+
800℃ GBEL growth (TC×5).

$Al_xGa_{1-x}As$ GBEL at 800 ℃ in sequence (c). The substrate temperature of the main growth was 750 ℃. A graded-bandgap-layer of $Al_xGa_{1-x}As$ was grown between the $Al_{0.8}Ga_{0.2}As$ window layer and the p-GaAs emitter layer. Al content of $Al_xGa_{1-x}As$ is varied linearly with the distance from the window layer (x varies from 0.29 to 0). The common earth electrodes of top and bottom cell were formed with AuSb/Au on the surface of n^+-Si layer. The electrodes for out-put of top cell and bottom cell were made of AuZn/Au and Au at p^+-GaAs cap layer and the p^+-Si back layer, respectively. The patterns of surface electrode on p^+-GaAs cap layer are shown in Fig.3-2. The double antireflection films are consisted of ZnS and MgF_2 film evaporated by the electron-beam evaporation. The total area of the solar cell is 5x5 mm^2 for the top cell and the bottom cell. The defect density of the GaAs solar cell on Si was evaluated by the electron-beam-induced current image. The conversion efficiency (η) and the short-circuit current (Jsc) are the active area values.

3-2-3. Structure of the tandem solar cell

The schematic cross-sectional structure of the three-terminal GaAs/Si solar cell is shown in Fig. 3-3.

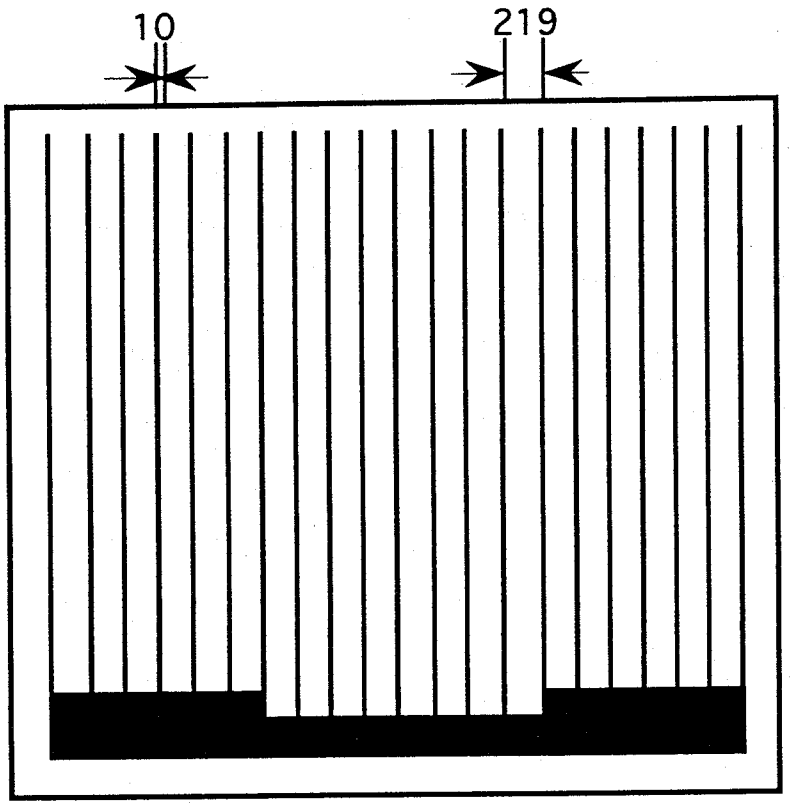

Total Area: 25.0 (mm^2)
Area of electrode: 3.00 (mm^2)
Effective area: 22.0 (mm^2)

(a)

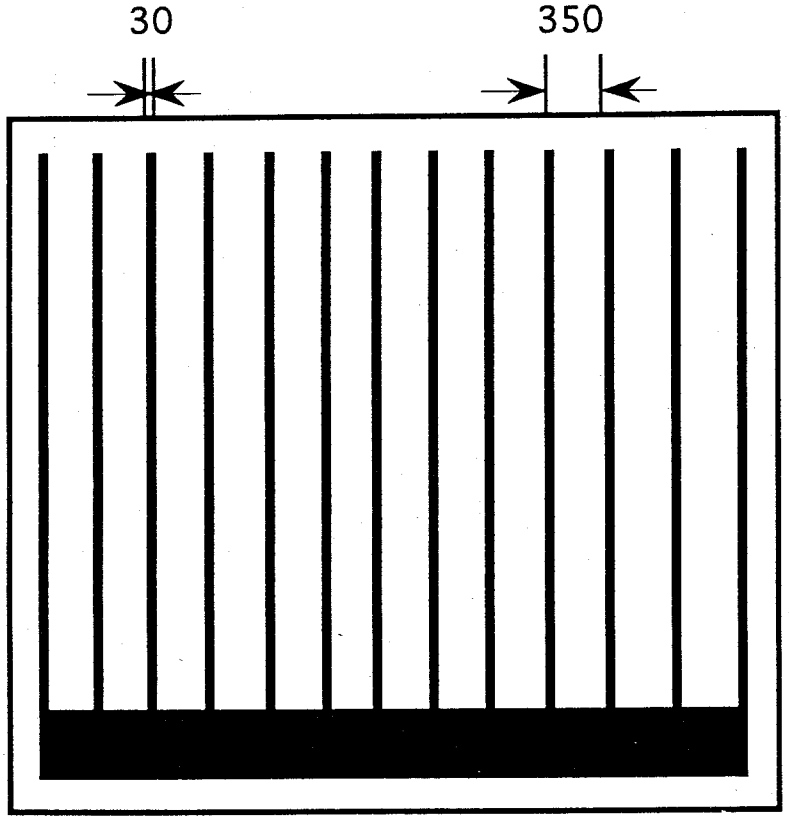

Total Area: 25.0 (mm^2)
Area of electrode: 3.89 (mm^2)
Effective area: 21.1 (mm^2)

(b)

Fig.3-2 The pattern of surface electrode of the GaAs/Si tandem solar cell.

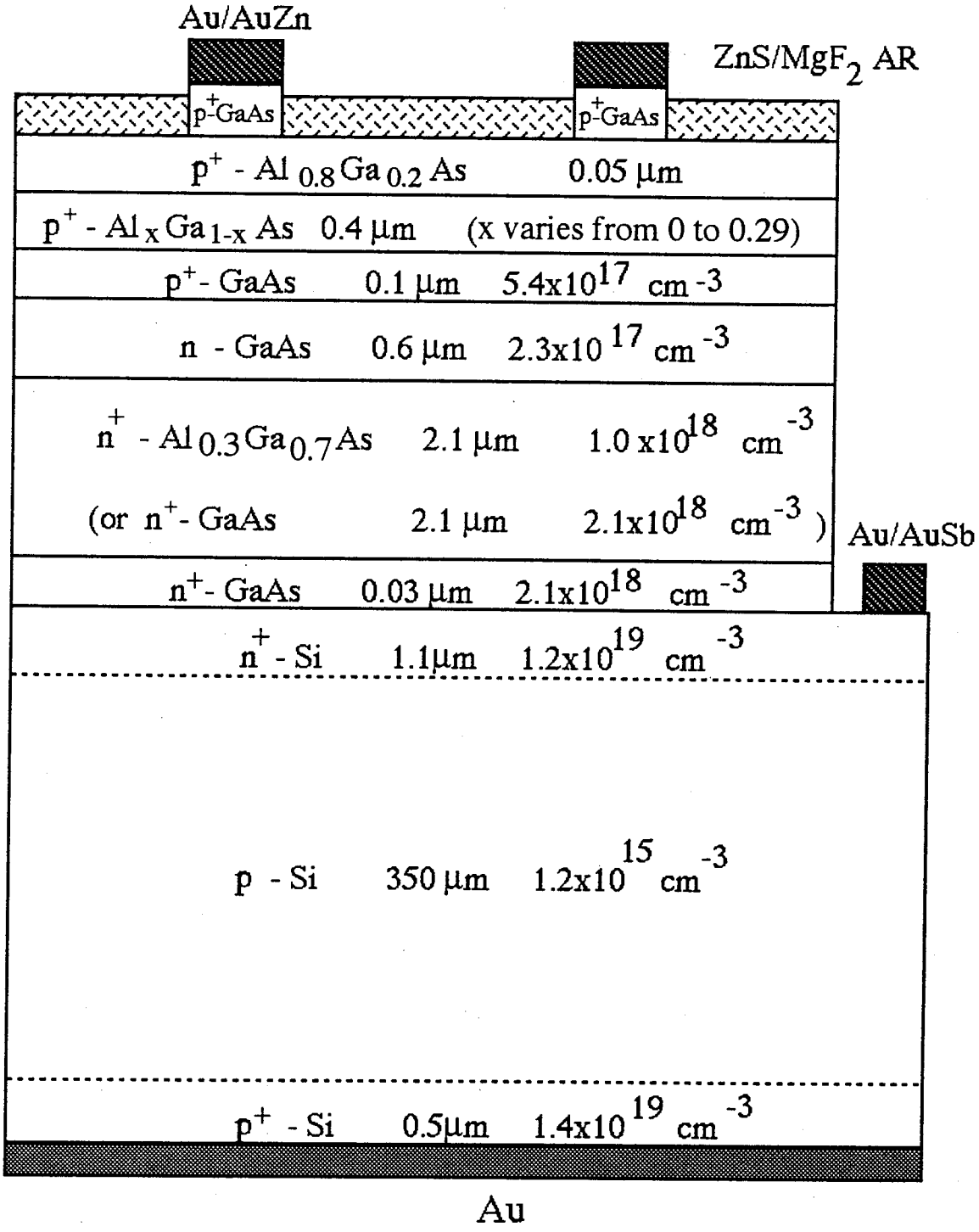

Fig.3-3 The schematic cross-sectional structure of the GaAs/Si three-terminal monolithic tandem solar cell.

3-3 Effects of GaAs growth on Si bottom cell

3-3-1 As auto-doping effect

During GaAs growth on Si with the atmosphere of AsH_3 and H_2, As diffused from the GaAs heteroepitaxial layer into the Si substrate, the top of the p-Si substrate is changed to an n-type. So an n-p junction is formed naturally with this procedure. We call it "As auto-doping". In order to investigate the As auto-doping effect, 3 μm-thick GaAs layer was grown on p-Si substrate. The evaluation of As diffusion depth in Si substrate was made by EBIC and secondary ion mass spectroscopy (SIMS) after etching off the GaAs layer. This n^+-Si layer with As auto-doping has a carrier concentration of 1.1×10^{19} cm^{-3} and a thickness of 1.0 μm. The I-V characteristics of this "As auto-doping" n^+-p Si solar cell is shown in Fig.3-4. It represents poorer performance of Si solar cell relative to that fabricated by the thermal diffusion method. The conversion efficiency is near to 7% (AM0, without antireflection). The profile of As and Ga diffusion can be seen from Fig.3-5. The depth of As diffusion is about 350 nm.

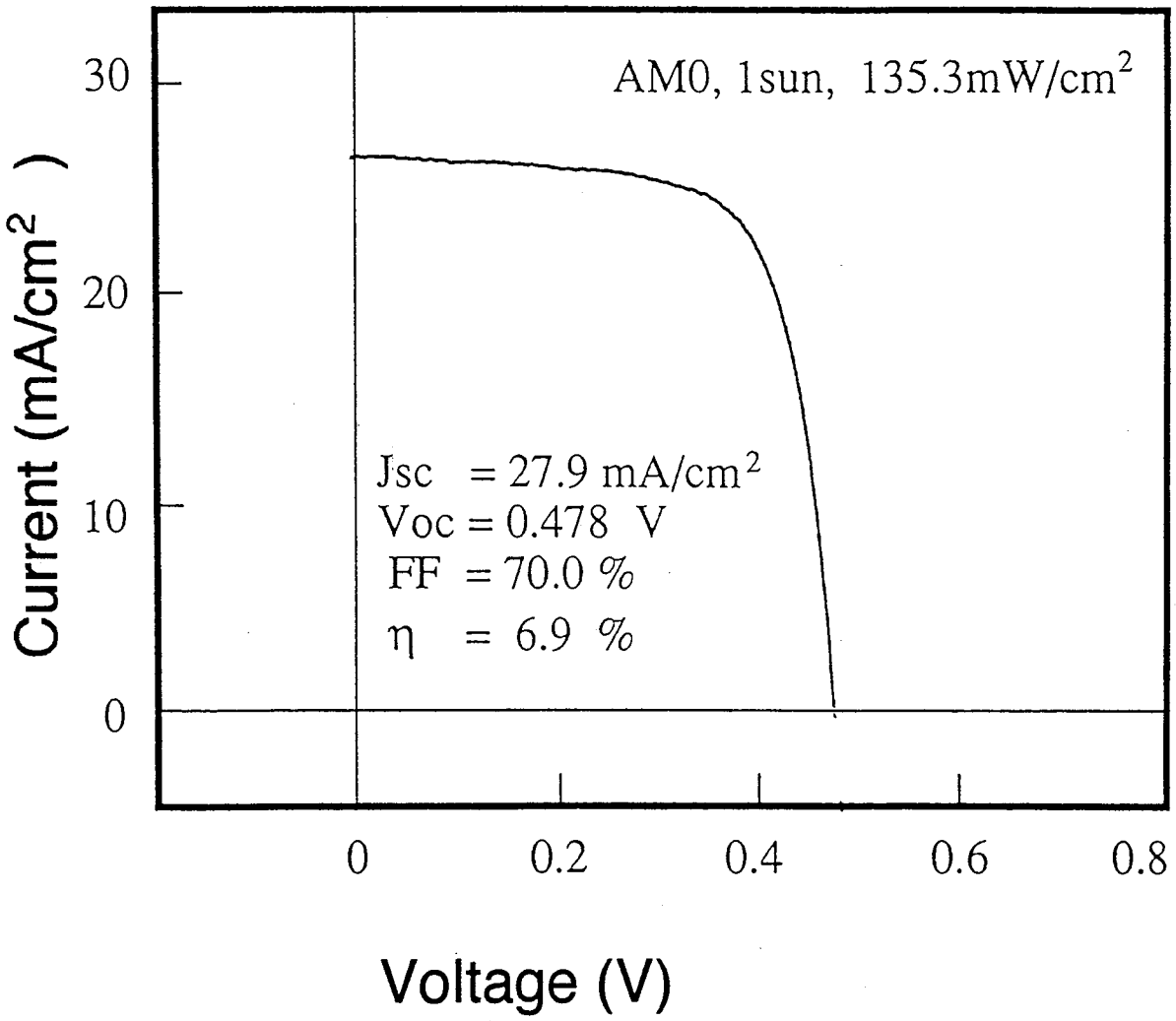

Fig.3-4 Current-voltage characteristics of "As auto-doping" for n-p Si solar cell (without antireflection films).

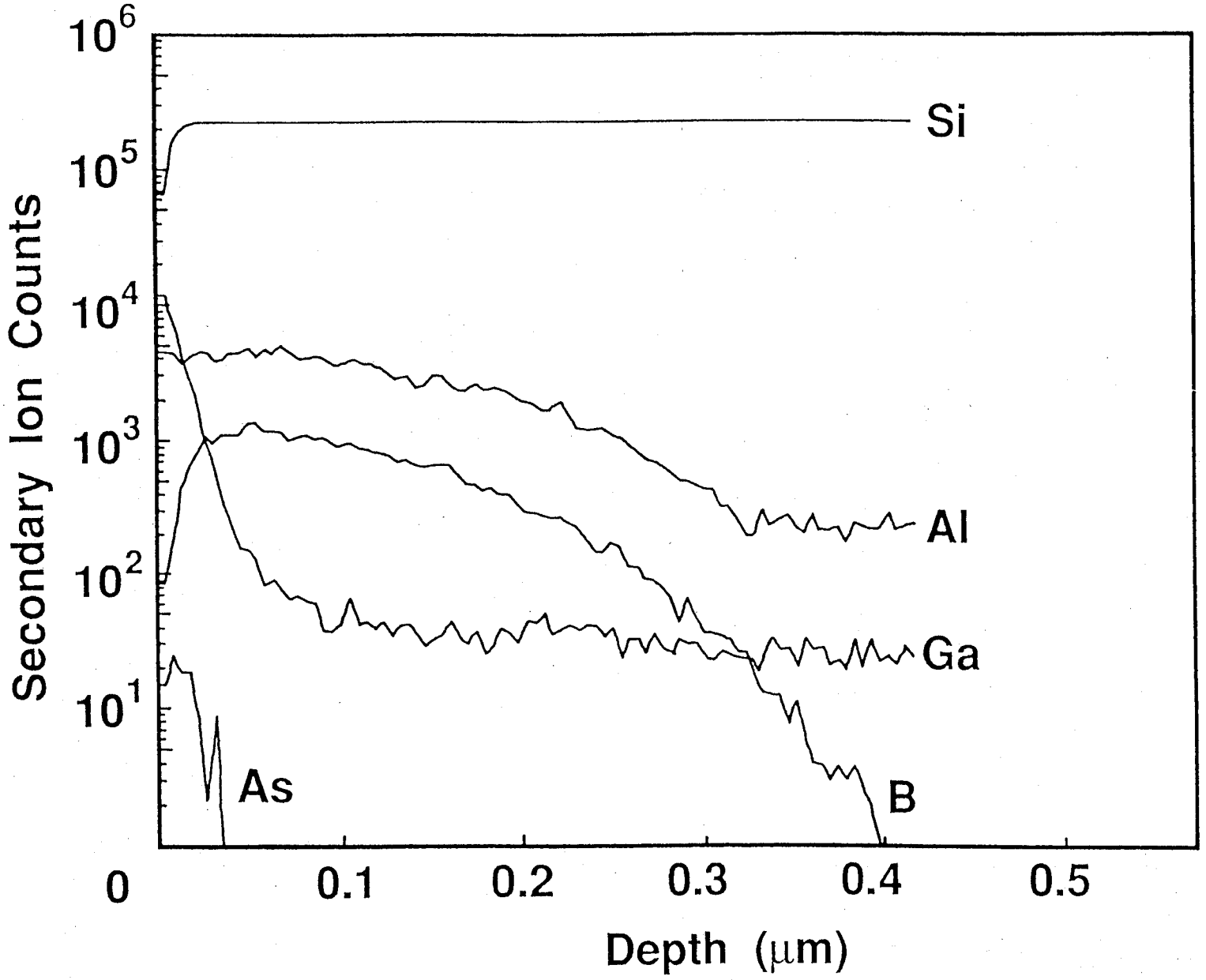

Fig.3-5 SIMS measurement on the "As auto-doping" for p-Si substrate

3-3-2 Properties of the Si bottom cell after GaAs growth

Prior to the epitaxial growth, using a p-Si substrate with resistance of 1.6 Ω·cm, an n^+-p junction of Si was formed by P-thermal diffusion method at 900 °C for the bottom cell of the tandem solar cell. The carrier concentration and thickness of n^+-Si layer are 2.6×10^{19} cm^{-3} and 0.5 μm, respectively. After GaAs was grown on it, the carrier concentration and the thickness of n^+-Si layer were changed to 1.4×10^{19} cm^{-3} and 1.1 μm, respectively. The measurements were made by four-point probe method and electron-beam-induced-current (EBIC) method, respectively. Fig.3-6 shows the I-V characteristics of the n^+-p Si solar cell before GaAs growth (A) and after GaAs growth (B and C). Conversion efficiency of 16.4% (AM0, 27 ℃) was obtained for n^+-p Si solar cell before GaAs growth, which corresponds to curve A in Fig.3-6. When the GaAs layers were grown and removed from the Si substrates having an n^+-p junction, the conversion efficiency of the Si solar cell changed a little for TCA 300～850 ℃ (curve B). But the efficiency of the Si solar cell was reduced to 12.5% with TCA 300～900 ℃ (curve C).

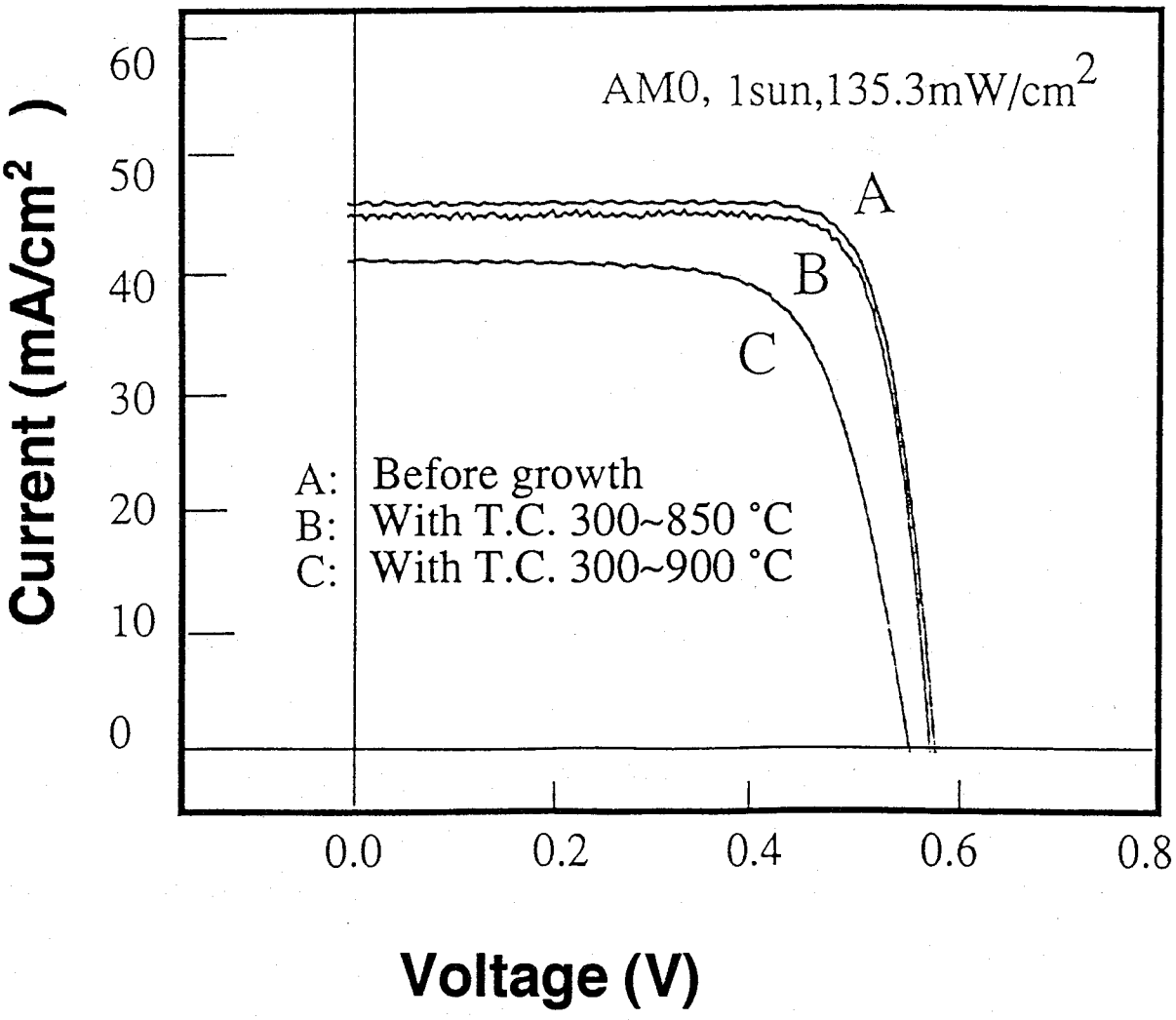

Fig.3-6 Current-voltage characteristics of the n^+-p Si solar cell (with ZnS/MgF_2 antireflection films).

3-4. Photovoltaic properties

3-4-1. GaAs top cell, Si bottom cell and the connection

3-4-1-1. GaAs top cells

Because of the existence of high-dislocation density in GaAs/Si, which degrades the lifetime of photo-generated carriers, GaAs solar cell on Si has a lower Jsc in comparison with GaAs solar cells on GaAs. One of the method to improve the efficiency is to use the electric field to collect the carriers. Inserting a graded-bandgap-layer of $Al_xGa_{1-x}As$ between the $Al_{0.8}Ga_{0.2}As$ window layer and the p-GaAs emitter layer, Al content of $Al_xGa_{1-x}As$ is varied linearly with the space distance from the window layer. It provides an electric field $E = -\frac{1}{q}\frac{\partial}{\partial y}[Eg(x,y)]$ [8] in the p-active region to enhance the collection of photo-generated carriers. Here q is magnitude of an electronic charge, x and y are aluminum mole fraction and distance from the $Al_{0.8}Ga_{0.2}As/Al_xGa_{1-x}As$ interface, respectively. The Al mole fraction at the surface of GBEL is taken to be 0.29, because the diffusion length [9], the electron mobility [10] and the lifetime [11] do not strongly depend on Al composition of $Al_xGa_{1-x}As$ in the range $x<0.3$. GBEL in the p-$Al_xGa_{1-x}As$ active layer (x varying from 0.29 to 0) will produce a strong electric field to reduce the effect of the surface recombination for the enhancement of the carrier collection efficiency effectively [12].

Fig. 3-7 shows the quantum efficiency of GaAs solar cell with and without GBEL. The quantum efficiency of the GaAs top

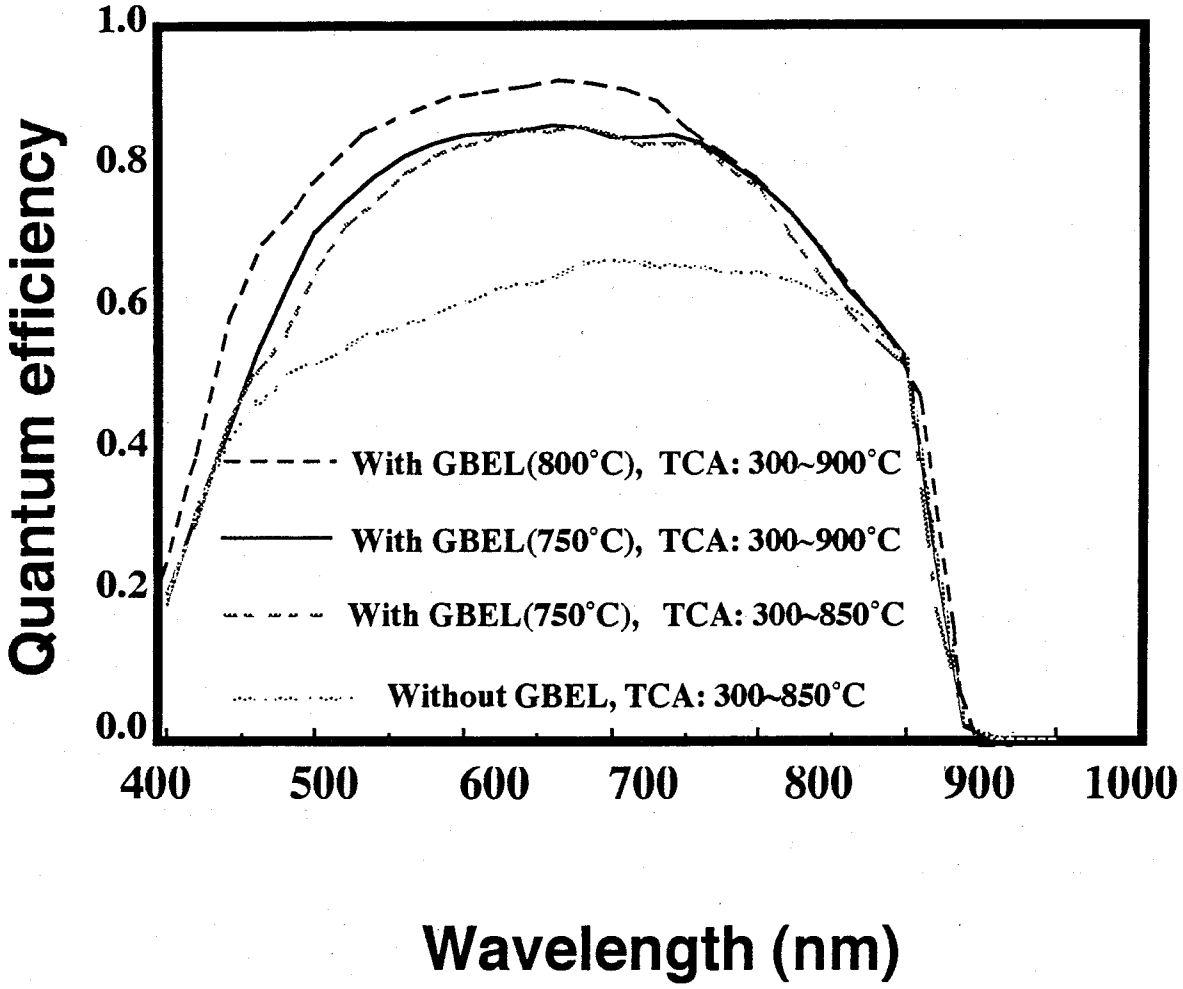

Fig.3-7 The quantum efficiencies of the GaAs top solar cells.

cell is improved clearly in wavelength from 460 nm to 860 nm comparing with the GaAs top cell on Si without the GBEL. This figure also indicates that the quantum efficiency of the solar cell with TCA 300～900℃ is higher than that of with TCA 300～850℃.When the GBEL of AlGaAs was grown at temperature of 800 ℃ , the quantum efficiency was improved further. Fig.3-8 is the EBIC images of the GaAs top cell with different temperatures of TCA, and it shows that TCA 300 ～ 900 ℃ (DSD=6.3×10^{6} cm^{-2}) treatment has better effect than that of TCA 300～850 ℃ (DSD=8.3×10^{6} cm^{-2}). Table 3-1 shows Jsc, Voc, FF and efficiency of the solar cell with various growth sequences. From this table, it can be seen that GBEL is only effective for improving the carrier collection efficiency and resulted in increase of Jsc. The effect was not observed for Voc, which is still limited by the high-dislocation density. These dislocations in GaAs epitaxial layer on Si not only degrade the lifetime of the minority carriers but also increase the dark-current of the GaAs top solar cell, which resulted in lower Voc [13]. Combining 300～900℃ TCA and the high temperature growth of the GBEL, the conversion efficiency of the GaAs top cell which is summarized in Table 3-1 is up to 15.9 % (AM0, 27 ℃) and Jsc=33.9 mA/cm^{2} was achieved. The current-voltage characteristics were measured under AM0 condition (1sun, 135.3mW/cm^{2}, 27 ℃) with a solar simulator.

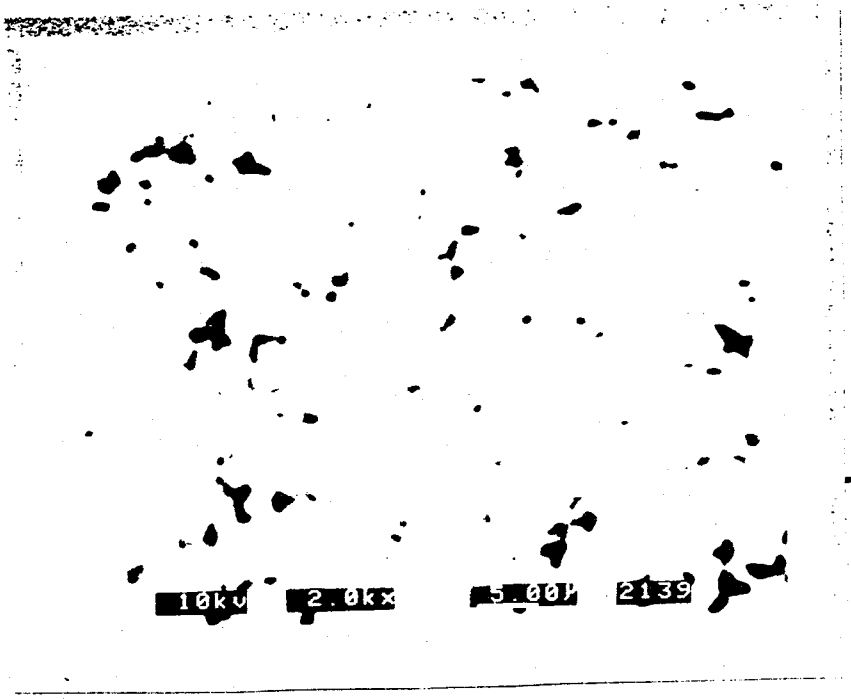

TCA: 300 ~850°C

DSD=8.3×10^{6} cm^{-2}

(a)

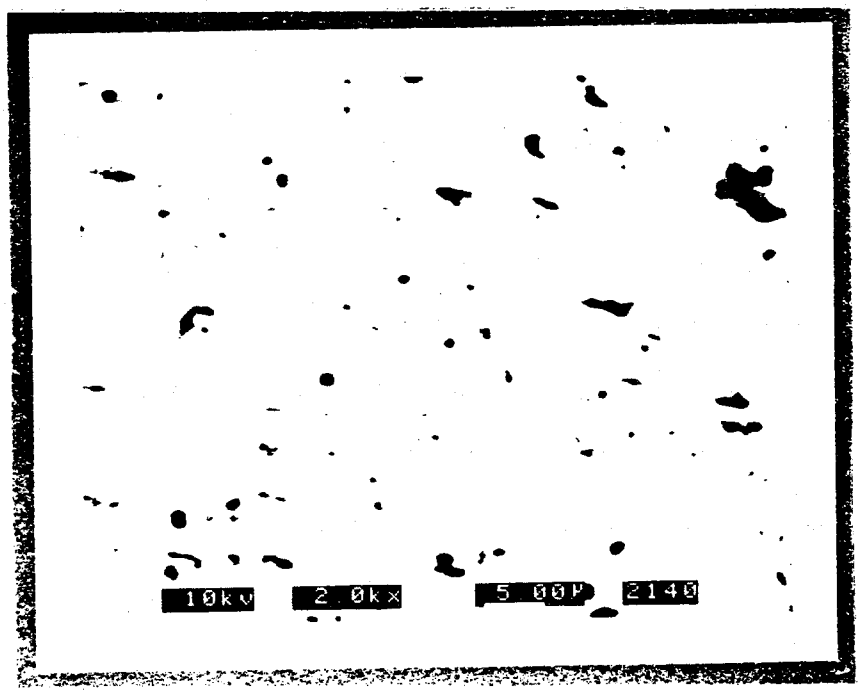

TCA: 300 ~900°C

DSD=6.3×10^{6} cm^{-2}

(b)

Fig.3-8 EBIC images of the GaAs top solar cells on Si substrates.

Table 3-1
Current-voltage data of the GaAs top cells on Si with different growth sequences.

Growth sequence	Jsc(mA/cm^2)	Voc(V)	FF (%)	η (%)
(a): Without GBEL	21.1	0.820	76.8	11.6
(a): With GBEL (750℃)	29.8	0.825	76.2	13.9
(b): With GBEL (750℃)	30.7	0.857	77.9	15.1
(c): With GBEL (800℃)	33.9	0.849	75.0	16.0

3-4-1-2. Si bottom cells

Since GaAs is a direct band-gap material, the absorption coefficient is so large that most of the photo-absorption and carrier generation processes in GaAs occur within 2 μm of the surface at the band edge. [8] Light of wavelength beyond 0.87 μm will penetrate into the GaAs film to the Si bottom cell in the case of GaAs/Si tandem cells. Therefore, the contribution of the Si bottom cell to the GaAs/Si tandem solar cell mainly occurs in the long wavelength region, and the improvement of quantum efficiency of the Si bottom cell in the long wavelength region is very important for the GaAs/Si tandem solar cell.

The effect of resistivity of the p-Si substrate on the Si bottom cell was analyzed theoretically in Chapter 2. In experiment, Si solar cells with the n^+-p-p^+ structure were fabricated using different resistivities by the same process. The photovoltaic characteristics of these solar cells in Table 3-2 show that when the resistivity of the Si substrate

increases, open-circuit voltage (Voc) decreases, but Jsc increases.

Table 3-2
Photovoltaic characteristics of the Si solar cell with various resistivity from 0.1 Ω·cm to 10 Ω·cm.

Resistivity (Ω·cm)	Jsc(mA/cm^2)	Voc(V)	FF (%)	η (%)
10	33.8	0.527	75.0	9.87
5.2	32.4	0.547	74.4	9.73
1.6	30.7	0..563	78.1	9.77
0.1	22.5	0.591	81.0	7.95

Therefore, the conversion efficiencies are almost same, i.e., near 10% (AM0, without front surface passivation and antireflection films) except for the solar cell with the substrate of which resistivity is 0.1 Ω-cm. The quantum efficiencies of these Si solar cells are quite different in the long wavelength region as shown in Fig.3-9. The n^+-p-p^+ of Si solar cell using substrate with the resistivity of 10 Ω-cm appears to have the best collection efficiency in the wavelength region from 800 nm to 1200 nm, which coincide with the theoretical result in the Chapter 2. This property is suitable for the bottom cell.

In order to clarify the effects of resistivities of Si on the GaAs/Si tandem solar cell, the GaAs top cells were fabricated on the Si solar cells with the resistivity of 1.6 Ω-cm and 10 Ω-cm. Figure 3-10 shows the I-V characteristics (a) and the quantum efficiencies(b) of the Si bottom cell.

Although the conversion efficiency of the Si (1.6 Ω-cm) solar cell is almost the same as that of the Si (10 Ω-cm) solar cell before GaAs growth (Table 3-2), the efficiency of the former is lower than that of the latter under the GaAs top cell. The efficiencies of the Si (1.6 Ω-cm) and Si (10 Ω-cm) solar cells with the GaAs top solar cells are 3.9% and 4.3% (AM0), respectively.

Table 3-3
Photovoltaic characteristics of the Si bottom cells with the GaAs top cells.

Buffer layer	Resistivity (Ω-cm)	Jsc (mA/cm^2)	Voc (V)	FF (%)	η (%)
GaAs	1.6	13.4	0.533	75.0	3.92
GaAs	10	14.3	0.522	78.0	4.31
AlGaAs	10	18.0	0.536	74.5	5.33

Using $Al_{0.3}Ga_{0.7}As$ buffer layer instead of the GaAs buffer layer, the efficiency of the Si bottom cell is increased to 5.3%. The I-V data are shown in Table 3-3.

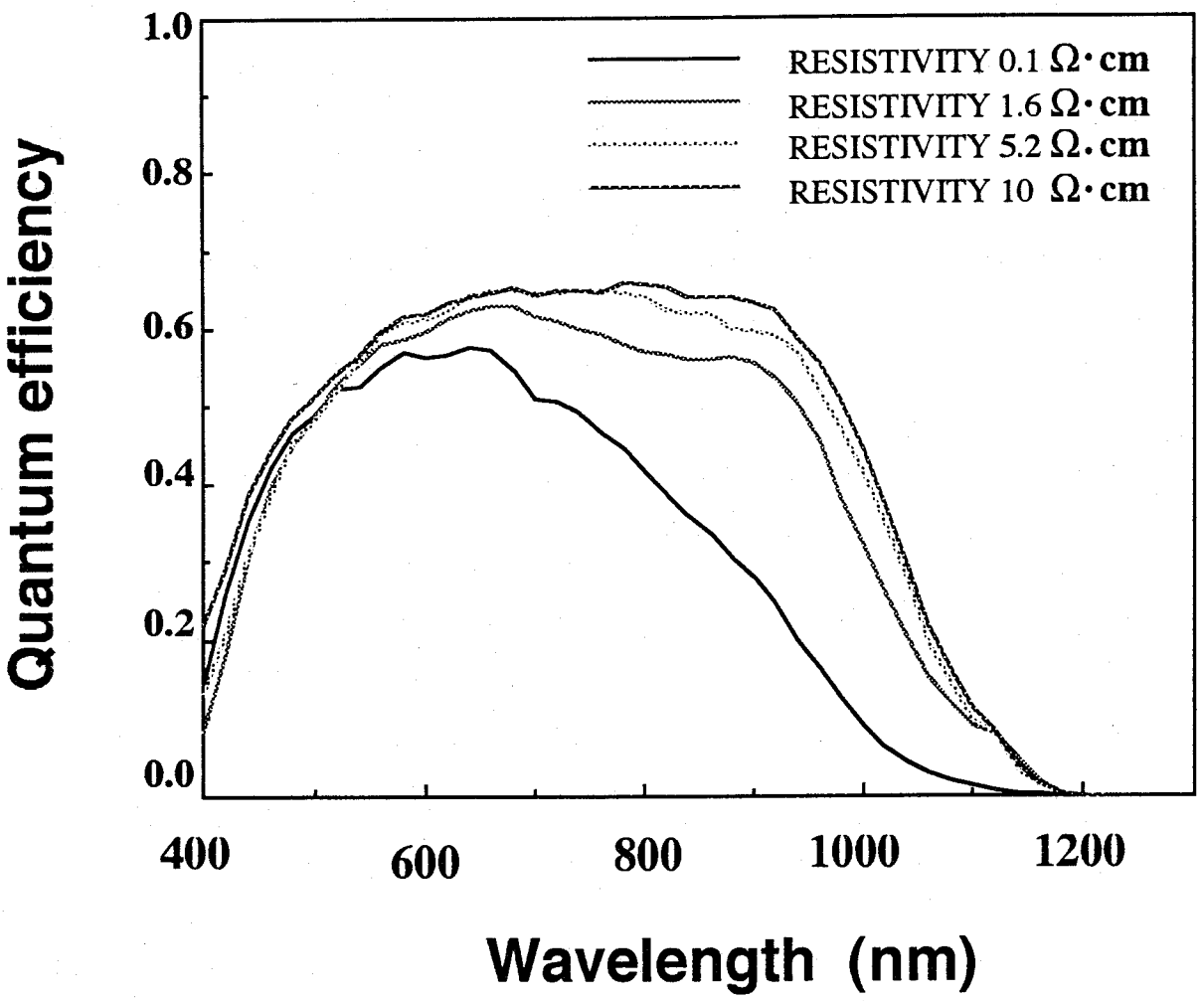

Fig.3-9 The quantum efficiences of Si solar cell with various substrate resistivities.

3-4-1-3. Connection between the top cell and bottom cell

For the GaAs/Si three-terminal tandem solar cell, there is an isotype n-n/ GaAs-Si heterojunction between the GaAs top cell and the Si bottom cell. In an n-n heterojunction, the conduction-band potential barrier is determined by the electron affinity difference for two semiconductors ($\Delta Ec=\chi_2-\chi_1$) and by the doping levels of semiconductors.[14] The band structure of the isotype GaAs-Si heterojunction is shown in Fig.3-11. In this study, the doping concentrations are very high in both the n^+-GaAs layer and n^+-Si layer near the GaAs/Si interface, and the energy step at the n-n heterojunction of GaAs/Si from electron affinity consideration is quite small, $\Delta Ec=0.06eV$ (χ_{GaAs} = 4.07eV, χ_{Si} = 4.01eV). Thus, the n-n/GaAs-Si heterojunction behaves as a resistance, and the resistance per unit area of the heterojunction is small enough to neglect in comparison with the series resistance of the GaAs top cell and the Si bottom cell.

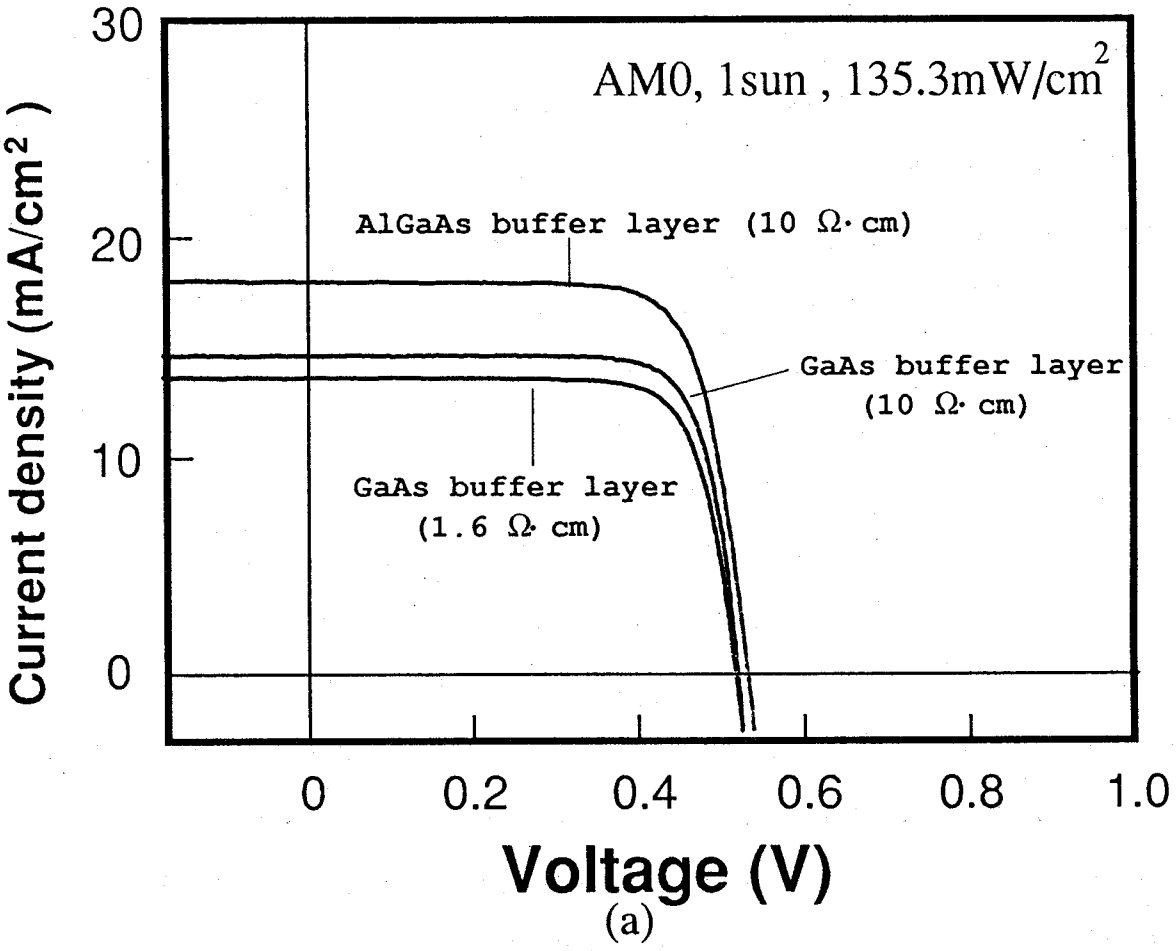

(a)

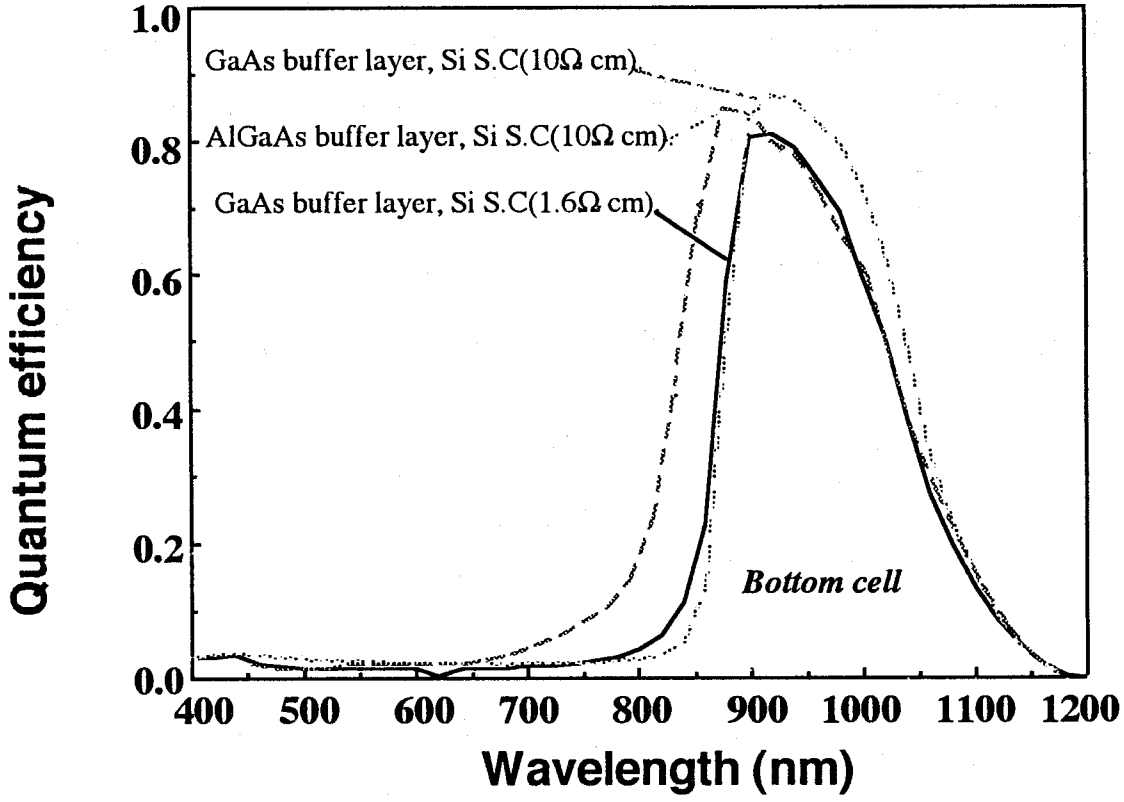

(b)

Fig.3-10 I-V characteristics and quantum efficiencies of the Si bottom cell under the GaAs and AlGaAs buffer layer.

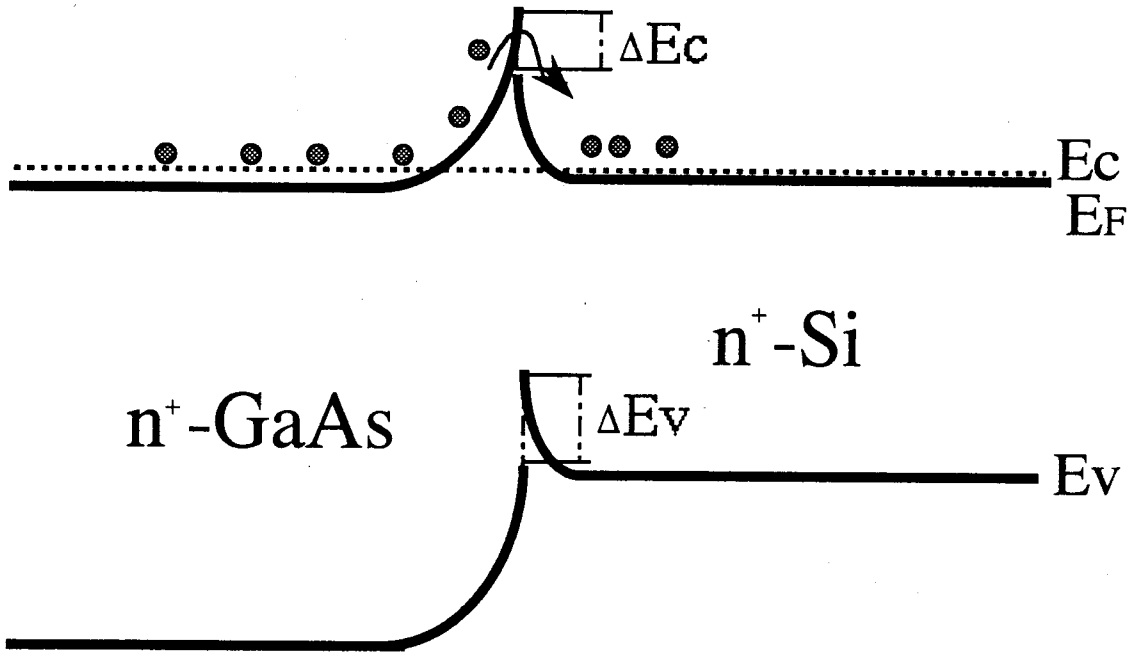

Fig.3-11 The band structure of the isotype n-n GaAs-Si heterojunction.

3-4-2. Photovoltaic properties of the tandem solar cell

Two kinds of the GaAs/Si tandem solar cells were fabricated and analyzed. One (**B** tandem solar cell) is that the GaAs top cell with a $Al_{0.3}Ga_{0.7}As$ buffer layer grown by using growth sequence (B) and the Si bottom cell made by a p-Si substrate with resistivity of 10 Ω·cm. Another (**C** tandem solar cell) is that the GaAs top cell with a GaAs buffer layer grown by using growth sequence (c) and the Si bottom cell made by a p-Si substrate with resistivity of 1.6 Ω·cm.

The quantum efficiencies of **B** and **C** tandem solar cell are shown in Fig.3-12. Using an $Al_{0.3}Ga_{0.7}As$ buffer layer between the top cell and the bottom cell, the spectral response of the Si bottom cell has a forward shift to the short wavelength direction. It is expected that the efficiency of the bottom cell increases because more incident light penetrates to the bottom cell since the band-gap energy of $Al_{0.3}Ga_{0.7}As$ is larger than that of GaAs. The experimental results show that the increase of the efficiency of the bottom cell from 3.90 % (**C** tandem solar cell) to 5.33% (**B** tandem solar cell), but the efficiency of the GaAs top cell is decreased from 16.0% to 14.2%.

For **C** tandem solar cell, the incident light is almost completely absorbed by the 3 μm-thick GaAs top cell in the wavelength region below the energy band edge of GaAs. The Si bottom solar cell (1.6 Ω·cm) has the efficiency of 3.9% only. The I-V characteristics of the GaAs top cell and the Si bottom cell are shown in Fig.3-13. The total conversion efficiency, 19.9% (AM0, the active area efficiency) of the **C** tandem solar

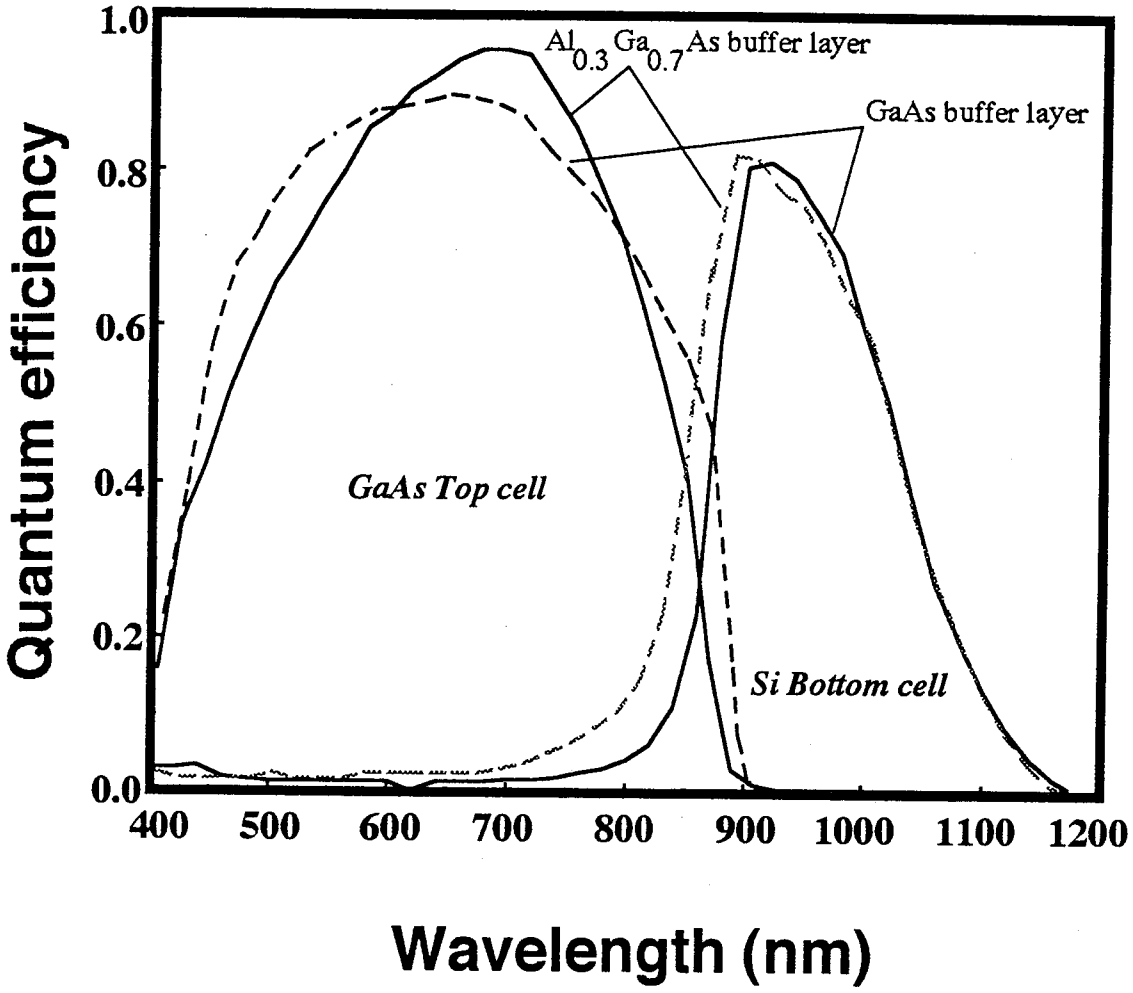

Fig.3-12 Quantum efficiencies of the GaAs/Si tandem solar cells with $Al_{0.3}Ga_{0.7}As$ and GaAs buffer layer.

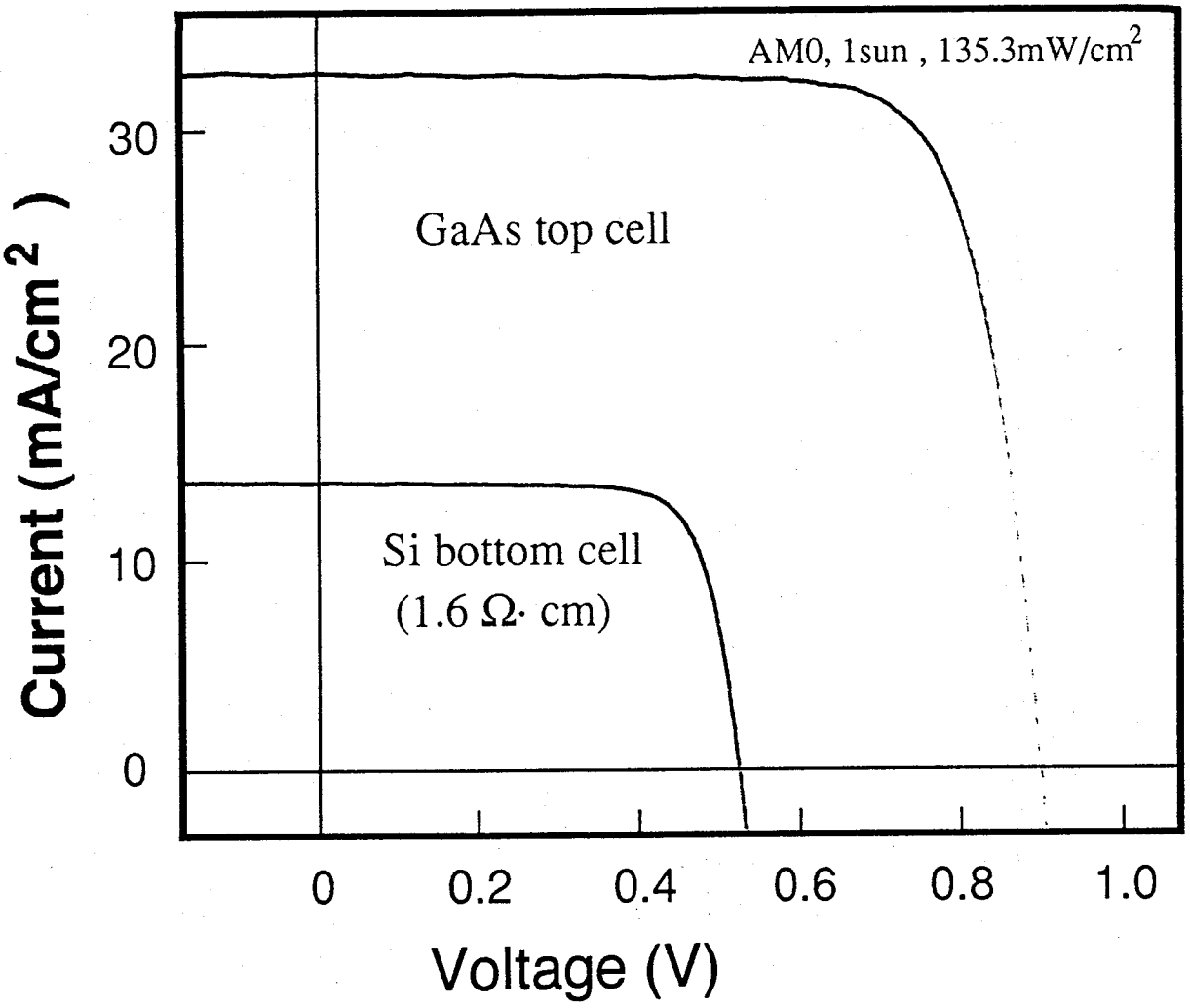

Fig.3-13 Current-voltage characteristics of the GaAs/Si tandem solar cell.

cell was achieved in combining the efficiency of the GaAs top cell (16.0%). The photovoltaic characteristics of the **B** tandem solar cell and **C** tandem solar cell are shown in Table 3-4.

Table 3-4
Photovoltaic properties of the GaAs/Si bottom cells with the GaAs and $Al_{0.3}Ga_{0.7}As$ buffer layer (η: the active-area efficiency).

Buffer layer	Cell	Jsc (mA/cm^2)	Voc (V)	FF (%)	η (%)
$Al_{0.3}Ga_{0.7}As$	GaAs top cell	33.1	0.819	71.0	14.2
	Si bottom cell	18.0	0.536	74.5	5.33
GaAs	GaAs top cell	33.9	0.849	75.0	16.0
	Si bottom cell	13.7	0.520	74.0	3.90

3-5 Conclusion

GaAs/Si three-terminal monolithic tandem solar cells fabricated by MOCVD were studied.

First, the "As auto-doping effect in Si" during GaAs growth on Si substrate were analyzed by the SIMS and EBIC. The Si solar cell with the n-p junction formed naturally during the growth has a poor performance, which is not suitable for the Si bottom cell.

Next, the effects of the GaAs growth on the Si bottom cells were investigated in comparison with the properties of the Si solar cells before and after GaAs growth. Application of the thermal treatment (300~900 ℃) improves the quality of GaAs film grown on Si, but it decreases the efficiency of the Si bottom solar cell from 16.4% to 12.5%.

Then, analyses on the properties of the GaAs top cell, the Si bottom cell and the connection between the top cell and the bottom cell were carried out, respectively. Using a graded-bandgap-layer of $Al_xGa_{1-x}As$, the quantum efficiency of GaAs top cell was considerably improved within wavelength from 460 nm to 860 nm. Short-circuit current of the GaAs top cell increased from 21.1 mA/cm^2 to 30.7 mA/cm^2. This effect was not observed for Voc. It can be thought that the GBEL structure is effective for improving the carrier collection and results in an increase in the short-circuit current density (Jsc), but not effective for increasing the open-circuit voltage (Voc) clearly, which is still limited by the high-dislocation density. The performance of the GaAs top

cell has been improved further when the GBEL structure of AlGaAs is growth at 800 ℃, the conversionøn efficiency is up to 16% (AM0, active-area efficiency).

For the Si bottom cell, the quantum efficiency in the long wavelength is enhanced by using p-Si substrate with proper resistivity (10 Ω·cm) and BSF structure. Instead of the GaAs buffer layer with $Al_{0.3}Ga_{0.7}As$ buffer layer, the efficiency of the Si bottom cell increases from 3.9% to 5.3%. And then, the characteristics of the connector between the top cell and the bottom cell are analyzed. An isotype n-n/ GaAs-Si heterojunction connector for the three-terminal GaAs/Si behaves as a resistance with very small value.

Finally, the experimental results of the GaAs/Si tandem solar cell were demonstrated. The total conversion efficiency (active-area efficiency) of 19.5% and 19.9% under 1 sun, AM0 measurement conditions have been achieved by the GaAs/Si three-terminal monolithic tandem solar cell with the GaAs and the AlGaAs buffer layer,respectively.

References

1) B.-C. Chung, G. F. Virshup, S. Hikido and N. R. Kaminar: Appl. Phys. Lett. **55** (1989) 1741.

2) K. A. Bertness, S. R. Kurtz, D. J. Firedman, A. E. Kibbler C. Kramer and J. M. Olson: Appl. Phys. Lett. **65** (1994) 989.

3) J. C. C. Fan, B-Y. Tsaur and B. J. Palm: *Conf. Rec. 16th IEEE Photovoltaic Specialists Conf.* (San Diego, USA,1982) p.692.

4) M. Yamaguchi: *Proc. Intern. PVSEC-6.* (Oxford, New Delhi, India, 1992) p503.

5) T. Nishioka, et al: *Tech. Digest Intern. PVSEC-3,* (Tokyo, Japan 1987) P-II-7.

6) M.Akiyama, Y.kawarad and K.Kaminish: Jpn. J. Appl. Phy. **23**. L843 (1984).

7) S. Nozaki, N. Noto, T. Egawa, A. T. Wu, T. soga, T. Jimbo and M. Umeno: Jpn. J. Appl. Phy, **29** (1990) 138.

8) H.J.Hovel: *Semiconductor and Semimetals*, Vol. 11. Solar Cells (Acamdemic Press, New York, 1975).

9) T. Kawakami: Jpn. J. Appl. Phys. **12**, (1973) 151.

10) A. A. Immorlica Jr. and G. L. Pearson: Appl. Phys. Lett. **25**. (1974) 570 .

11) H. Namizaki, M. Nagano and S. Nakahara: IEEE trans Electron Devices **ED-21**, (1974) 688.

12) M.Konagai and K.Takahashi: J. Appl Physics, **46**, (1975) 3542.

13) J. C. Zolper and A. M. Barnett: IEEE trans on Electron

Devices, **37**, (1990) 478.

14) A. G. Milens and D. L. Feucht: *Heterojunctions and Metal-Semiconductor Junctions* (Academic Press, New York, 1972).